Implementation of Discontinuous Galerkin Kirchhoff-Love Shells

Peter Kaufmann [*] ETH Zurich
Sebastian Martin [†] ETH Zurich
Mario Botsch [‡] Bielefeld University
Markus Gross [§] ETH Zurich

Abstract

This technical report describes an implementation of the discontinuous Galerkin (DG) finite element method for thin shells presented by [Noels and Radovitzky 2008]. After a short summary of the Kirchhoff-Love shell theory, the DG weak form is reviewed and the assembly of the stiffness matrix is described in detail. We also present a co-rotational extension to the method which allows us to simulate large rotational deformations without the typical linearization artifacts of a linear shell model. The proposed model has been successfully applied to the simulation of cutting and fracturing of thin shells by means of *harmonic enrichments* [Kaufmann et al. 2009].

1 Kirchhoff-Love Shell Mechanics

This section reviews the basic equations of the Kirchhoff-Love shell theory in order to establish the required notation and introduce quantities that will be referred to in subsequent sections. For another introduction to shell theory, we refer to [Cirak et al. 2000]. The detailed derivations of the thin-shell theory can be found in [Simo and Fox 1989].

The Kirchhoff-Love theory for thin shells makes two main assumptions. First, the height of the shell is assumed to be small compared to its overall size. Second, a vector normal to the shell that is transformed according to the local deformation of the shell always remains normal to the shell and un-stretched [Wempner and Talaslidis 2003]. The first assumption allows for first-order approximations in the direction normal to the shell, while the second assumption results in shearing deformations being neglected.

1.1 Shell Geometry

The deformation of a thin shell can be fully described by the deformation of its mid-surface, which is a two-dimensional surface embedded in $\mathbb{R}^3$. The shell extends up to distance $h/2$ from the mid-surface, where h is the height of the shell. The mid-surface is parameterized using coordinates $(\xi^1, \xi^2) \in \Omega \subset \mathbb{R}^2$, which allows us to define the current deformation of the shell using a function $\boldsymbol{\varphi}(\xi^1, \xi^2) : \Omega \to \mathbb{R}^3$. Similarly, the initial (undeformed) configuration of the shell is defined by a function $\boldsymbol{\varphi}_0(\xi^1, \xi^2)$.

The surface basis vectors (tangent vectors) of the deformed and undeformed configuration, respectively, can be computed as $\boldsymbol{\varphi}_{,\alpha}(\xi^1, \xi^2)$ and $\boldsymbol{\varphi}_{0,\alpha}(\xi^1, \xi^2)$. Note that here and in the following, Greek indices indicate values 1 and 2, while a comma denotes partial differentiation. For example, $\boldsymbol{\varphi}_{,\alpha}(\xi^1, \xi^2) = \frac{\partial \boldsymbol{\varphi}(\xi^1, \xi^2)}{\partial \xi^\alpha}$. In the following, the explicit dependency of these quantities on (ξ^1, ξ^2) will be dropped, so we simply write $\boldsymbol{\varphi}$ instead of $\boldsymbol{\varphi}(\xi^1, \xi^2)$.

As any normal to the shell surface will always stay normal to the shell under deformation, the deformed surface normal vector can be computed from the basis vectors as

$$\mathbf{t} = \frac{\boldsymbol{\varphi}_{,1} \times \boldsymbol{\varphi}_{,2}}{\|\boldsymbol{\varphi}_{,1} \times \boldsymbol{\varphi}_{,2}\|} \tag{1}$$

and similarly for the undeformed configuration. Together with $\boldsymbol{\varphi}_{,1}$ and $\boldsymbol{\varphi}_{,2}$, $\mathbf{t}$ defines a local coordinate system for a point (ξ^1, ξ^2) on the mid-surface of the shell.

The deformed configuration can also be described relatively to the undeformed configuration, using a displacement field $\mathbf{u} : \Omega \to \mathbb{R}^3$ that defines the displacement of each point on the mid-surface. The deformed configuration can thus be described as

$$\boldsymbol{\varphi} = \boldsymbol{\varphi}_0 + \mathbf{u}. \tag{2}$$

1.2 Shell Mechanics

In volumetric elasticity, the local deformation of a material point can be described using the Green strain tensor. Transforming this tensor into the coordinate system of the shell and using the fact that the height h of the shell is small, the first order approximation of the Green strain can be formulated as a sum of two distinct terms: the first term only depends on the local basis vectors (i.e., first derivatives of $\boldsymbol{\varphi}$), while the second one also depends on derivatives of the basis vectors and thus measures the local change in curvature. The first term is called the *stretching* or *membrane strain* tensor, while the second one is referred to as the *bending strain* tensor.

Describing the deformed configuration $\boldsymbol{\varphi}$ in terms of the displacement field $\mathbf{u}$ according to (2), to first order in $\mathbf{u}$ the membrane strain two-tensor ε becomes

$$\varepsilon_{\alpha\beta}(\mathbf{u}) := \frac{1}{2}(\boldsymbol{\varphi}_{0,\alpha} \cdot \mathbf{u}_{,\beta} + \mathbf{u}_{,\alpha} \cdot \boldsymbol{\varphi}_{0,\beta}). \tag{3}$$

Note that the dot $(\cdot)$ denotes a vector dot product and will only be used for this purpose. The bending strain two-tensor ρ becomes

$$\begin{aligned}
&\rho_{\alpha\beta}(\mathbf{u}) := \\
&\boldsymbol{\varphi}_{0,\alpha\beta} \cdot \mathbf{t}_0 \frac{1}{\bar{j}_0}(\mathbf{u}_{,1} \cdot (\boldsymbol{\varphi}_{0,2} \times \mathbf{t}_0) - \mathbf{u}_{,2} \cdot (\boldsymbol{\varphi}_{0,1} \times \mathbf{t}_0)) \\
&+\frac{1}{\bar{j}_0}(\mathbf{u}_{,1} \cdot (\boldsymbol{\varphi}_{0,\alpha\beta} \times \boldsymbol{\varphi}_{0,2}) - \mathbf{u}_{,2} \cdot (\boldsymbol{\varphi}_{0,\alpha\beta} \times \boldsymbol{\varphi}_{0,1})) \\
&-\mathbf{u}_{,\alpha\beta} \cdot \mathbf{t}_0.
\end{aligned} \tag{4}$$

In the above equation, $\bar{j}_0$ is the determinant of the Jacobian of the undeformed mid-surface, defined as

$$\bar{j}_0 := \|\boldsymbol{\varphi}_{0,1} \times \boldsymbol{\varphi}_{0,2}\|. \tag{5}$$

As daunting as these strain tensors might seem at first, note that quantities such as $\boldsymbol{\varphi}_0$, $\mathbf{t}_0$ and $\bar{j}_0$ depend on the undeformed configuration only and can thus be precomputed for any position (ξ^1, ξ^2).

Computing stresses from strains using a linear constitutive law, a formulation for the deformation energy can be found, which, by applying the variational principle, leads to the weak formulation

$$a(\mathbf{u}, \mathbf{v}) = f(\mathbf{v}), \tag{6}$$

[*] e-mail: peterkau@inf.ethz.ch
[†] e-mail: smartin@inf.ethz.ch
[‡] e-mail: botsch@techfak.uni-bielefeld.de
[§] e-mail: grossm@inf.ethz.ch

which must hold for all test functions $\mathbf{v} : \Omega \rightarrow \mathbb{R}^3$. The right-hand side $\mathbf{f}$ represents external forces, and the weak form $a(\mathbf{u}, \mathbf{v})$ is defined as

$$\begin{aligned} a(\mathbf{u}, \mathbf{v}) \quad &:= \quad \int_\Omega \epsilon_{\alpha\beta}(\mathbf{v}) \mathcal{H}_n^{\alpha\beta\gamma\delta} \epsilon_{\gamma\delta}(\mathbf{u}) \mathrm{d}A \\ &\quad + \int_\Omega \rho_{\alpha\beta}(\mathbf{v}) \mathcal{H}_m^{\alpha\beta\gamma\delta} \rho_{\gamma\delta}(\mathbf{u}) \mathrm{d}A. \end{aligned} \tag{7}$$

Note that Einstein sum notation is in effect here, meaning that repeated indices are summed over.

In the above weak form, $\mathcal{H}_n^{\alpha\beta\gamma\delta}$ and $\mathcal{H}_m^{\alpha\beta\gamma\delta}$ define the constitutive relations between stress and strain. They are defined as

$$\mathcal{H}_n^{\alpha\beta\gamma\delta} \quad := \quad \frac{Eh}{1-\nu^2} \mathcal{H}^{\alpha\beta\gamma\delta}, \tag{8}$$

$$\mathcal{H}_m^{\alpha\beta\gamma\delta} \quad := \quad \frac{Eh^3}{12(1-\nu^2)} \mathcal{H}^{\alpha\beta\gamma\delta}, \tag{9}$$

where

$$\begin{aligned} \mathcal{H}^{\alpha\beta\gamma\delta} \quad &:= \quad \nu(\boldsymbol{\varphi}_0^{,\alpha} \cdot \boldsymbol{\varphi}_0^{,\beta})(\boldsymbol{\varphi}_0^{,\gamma} \cdot \boldsymbol{\varphi}_0^{,\delta}) \\ &+ \quad \frac{1}{2}(1-\nu)(\boldsymbol{\varphi}_0^{,\alpha} \cdot \boldsymbol{\varphi}_0^{,\gamma})(\boldsymbol{\varphi}_0^{,\delta} \cdot \boldsymbol{\varphi}_0^{,\beta}) \\ &+ \quad \frac{1}{2}(1-\nu)(\boldsymbol{\varphi}_0^{,\alpha} \cdot \boldsymbol{\varphi}_0^{,\delta})(\boldsymbol{\varphi}_0^{,\gamma} \cdot \boldsymbol{\varphi}_0^{,\beta}). \end{aligned} \tag{10}$$

$\boldsymbol{\varphi}_0^{,1}$ and $\boldsymbol{\varphi}_0^{,2}$ denote the *contravariant basis vectors*. These can be computed as follows: defining the metric tensor as a 2×2 matrix

$$\mathbf{G} := \begin{pmatrix} \boldsymbol{\varphi}_{0,1} \cdot \boldsymbol{\varphi}_{0,1} & \boldsymbol{\varphi}_{0,1} \cdot \boldsymbol{\varphi}_{0,2} \\ \boldsymbol{\varphi}_{0,2} \cdot \boldsymbol{\varphi}_{0,1} & \boldsymbol{\varphi}_{0,2} \cdot \boldsymbol{\varphi}_{0,2} \end{pmatrix}, \tag{11}$$

compute

$$\begin{pmatrix} | & | \\ \boldsymbol{\varphi}_0^{,1} & \boldsymbol{\varphi}_0^{,2} \\ | & | \end{pmatrix} = \begin{pmatrix} | & | \\ \boldsymbol{\varphi}_{0,1} & \boldsymbol{\varphi}_{0,2} \\ | & | \end{pmatrix} \mathbf{G}^{-T}. \tag{12}$$

Note that the constitutive relations (8) and (9) also depend on the Young's modulus E and Poisson's ratio ν of the material.

2 Discontinuous Galerkin FEM Shells

The above weak form (7) could be discretized using a standard finite element approach [Hughes 2000; Zienkiewicz and Taylor 2000]. However, a closer look at the weak form reveals that due to the second derivatives in the bending strain, appropriate FEM basis functions must be able to reproduce C^1 continuous displacement fields [Hughes 2000]. Constructing fully compatible basis functions that provide the required degree of continuity across elements is problematic. A variety of approaches are in use, such as ignoring the continuity requirements or introducing additional variables, e.g. derivatives at edge mid-points [Zienkiewicz and Taylor 2000]. Other approaches use non-local interpolation schemes [Cirak et al. 2000].

A DG FEM approach for thin shells avoids the problem by only requiring basis functions that are C^0 across elements and enforcing C^1 continuity in a weak sense. The formulation results in additional integrals over element edges, which effectively introduce a deformation energy term which penalizes discontinuities in the derivatives.

In the case of DG FEM as described in [Noels and Radovitzky 2008], the weak form becomes

$$a^{DG}(\mathbf{u}, \mathbf{v}) := \sum_K a^K(\mathbf{u}, \mathbf{v}) + \sum_e a^e(\mathbf{u}, \mathbf{v}) \tag{13}$$

for elements K and interior edges e (edges with neighboring elements on both sides). a^K corresponds to the weak form (7) evaluated on element K. a^e is defined on interior edges as follows:

$$\begin{aligned} &a^e(\mathbf{u}, \mathbf{v}) := \\ &\int_e [\![\Delta\mathbf{t}(\mathbf{v})]\!] \cdot \boldsymbol{\varphi}_{0,\gamma} \nu_\delta^- \left\{ \mathcal{H}_m^{\alpha\beta\gamma\delta} \right\} [\![\Delta\mathbf{t}(\mathbf{u})]\!] \cdot \boldsymbol{\varphi}_{0,\alpha} \nu_\beta^- \eta^e \mathrm{d}s \\ &+ \int_e \left\{ \rho_{\alpha\beta}(\mathbf{v}) \mathcal{H}_m^{\alpha\beta\gamma\delta} \boldsymbol{\varphi}_{0,\gamma} \right\} \nu_\delta^- \cdot [\![\Delta\mathbf{t}(\mathbf{u})]\!] \, \mathrm{d}s \\ &+ \int_e [\![\Delta\mathbf{t}(\mathbf{v})]\!] \cdot \left\{ \rho_{\alpha\beta}(\mathbf{u}) \mathcal{H}_m^{\alpha\beta\gamma\delta} \boldsymbol{\varphi}_{0,\gamma} \right\} \nu_\delta^- \mathrm{d}s. \end{aligned} \tag{14}$$

Considering an edge e, element K^+ lies on the left-hand side of the directed edge and element K^- on the right-hand side. Quantities associated with either element are superscripted with a $-$ or $+$, respectively. $[\![\cdot]\!]$ is the jump operator, defined on the edge as

$$[\![\mathbf{v}]\!] := \mathbf{v}^+ - \mathbf{v}^-$$

and $\{\cdot\}$ the average operator, defined as

$$\begin{aligned} \{\mathbf{v}\} \quad &:= \quad \frac{1}{2}(\mathbf{v}^+ + \mathbf{v}^-) \\ \{v\} \quad &:= \quad \frac{1}{2}(v^+ + v^-) \end{aligned}$$

for $\mathbf{v} \in \mathbb{R}^3$ and $v \in \mathbb{R}$. η^e is a penalty factor for edge e which depends on a global penalty parameter η and the local element size as follows:

$$\eta^e = \frac{\eta}{h^e} \tag{15}$$

where h^e is the characteristic size of the edge. The characteristic size is computed from the areas and circumferences of the two adjacent elements using

$$h^e = \min\left(\frac{|A^+|}{|\partial A^+|}, \frac{|A^-|}{|\partial A^-|} \right). \tag{16}$$

In the above weak form, $\Delta\mathbf{t}(\mathbf{u})$ is the change of the normal vector, which can be computed as

$$\begin{aligned} \Delta\mathbf{t}(\mathbf{u}) \quad &= \quad \frac{1}{\bar{j}_0} \big(\boldsymbol{\varphi}_{0,1} \times \mathbf{u}_{,2} - \boldsymbol{\varphi}_{0,2} \times \mathbf{u}_{,1} \\ &\quad + \mathbf{t}_0 \, \mathbf{u}_{,1} \cdot (\mathbf{t}_0 \times \boldsymbol{\varphi}_{0,2}) \\ &\quad - \mathbf{t}_0 \, \mathbf{u}_{,2} \cdot (\mathbf{t}_0 \times \boldsymbol{\varphi}_{0,1}) \big). \end{aligned} \tag{17}$$

$\boldsymbol{\nu}^- = (\nu_1^-, \nu_2^-)^T$ is the outer unit normal of K^- represented in the *conjugate basis* $\boldsymbol{\varphi}_0^{,\alpha}$, see (12).

Note that the first term in (14) penalizes the *jump* of the *change* of the normal vector $\mathbf{t}$ on the edge. In other words, $[\![\Delta\mathbf{t}(\mathbf{u})]\!]$ is zero if the displacement field $\mathbf{u}$ changes the normals $\mathbf{t}^-$ and $\mathbf{t}^+$ on either side of the edge in the same way. The other two terms in (14) are responsible for making the formulation consistent and symmetric, see [Arnold et al. 2001].

3 Stiffness Matrix Assembly

This section describes in detail how the stiffness matrix $\mathbf{K}$ can be computed from element and edge contributions. We follow the formulation in [Noels and Radovitzky 2008], but from now on will employ Voigt notation in order to avoid tensor notation and provide a more tangible implementation. Although the formulation in Voigt notation may appear to be a bit awkward, it will hopefully be useful to people not familiar with tensor notation.

3.1 Basis Functions

The undeformed shell surface is defined in terms of basis functions $N^a : \Omega \rightarrow \mathbb{R}$ as

$$\boldsymbol{\varphi}_0 = \sum_a N^a \mathbf{X}_0^a, \tag{18}$$

where $\mathbf{X}_0^a \in \mathbb{R}^3$ is the initial position of node a. It follows that the undeformed surface basis vectors can be computed as

$$\boldsymbol{\varphi}_{0,\alpha} = \sum_a N^a_{,\alpha} \mathbf{X}_0^a, \tag{19}$$

by differentiating the basis functions N^a with respect to ξ^1 and ξ^2. Similarly, the displacement field $\mathbf{u}$ is discretized as

$$\mathbf{u} = \sum_a N^a \mathbf{u}^a \tag{20}$$

with nodal displacements $\mathbf{u}^a$.

As proposed in [Noels and Radovitzky 2008], we employ quadrangular elements with 8 nodes and bi-quadratic basis functions. The basis functions are:

$$\begin{aligned}
N^1 &= -\frac{1}{4}(-1+\xi^2)(-1+\xi^1)(\xi^1+\xi^2+1)\\
N^2 &= -\frac{1}{4}(-1+\xi^2)(1+\xi^1)(\xi^1-\xi^2-1)\\
N^3 &= \frac{1}{4}(1+\xi^2)(1+\xi^1)(\xi^1+\xi^2-1)\\
N^4 &= \frac{1}{4}(1+\xi^2)(-1+\xi^1)(\xi^1-\xi^2+1)\\
N^5 &= \frac{1}{2}(1-\xi^1\xi^1)(1-\xi^2)\\
N^6 &= \frac{1}{2}(1-\xi^2\xi^2)(1+\xi^1)\\
N^7 &= \frac{1}{2}(1-\xi^1\xi^1)(1+\xi^2)\\
N^8 &= \frac{1}{2}(1-\xi^2\xi^2)(1-\xi^1)
\end{aligned}$$

for element coordinates (ξ^1, ξ^2) with $-1 \leq \xi^1, \xi^2 \leq 1$.

When working with triangular 6-node elements, the following quadratic basis functions can be used

$$\begin{aligned}
N^1 &= 1 - 3\xi^1 - 3\xi^2 + 2\xi^1\xi^1 + 4\xi^1\xi^2 + 2\xi^2\xi^2\\
N^2 &= \xi^1(2\xi^1 - 1)\\
N^3 &= \xi^2(2\xi^2 - 1)\\
N^4 &= -4\xi^1(-1 + \xi^1 + \xi^2)\\
N^5 &= 4\xi^1\xi^2\\
N^6 &= -4\xi^2(-1 + \xi^1 + \xi^2)
\end{aligned}$$

where $\xi^1, \xi^2 \geq 0$ and $\xi^1 + \xi^2 \leq 1$. The node numbering for the two elements is depicted in Fig. 1.

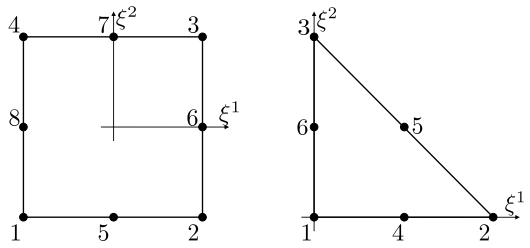

Figure 1: *Node numbering for the quadrangular (left) and triangular element (right).*

3.2 Assembly

Element Contributions. Similar to [Cirak et al. 2000], we represent the membrane strain two-tensor in Voigt notation as

$$\hat{\varepsilon} := \begin{pmatrix} \varepsilon_{11} \\ \varepsilon_{22} \\ \varepsilon_{12} + \varepsilon_{21} \end{pmatrix}. \tag{21}$$

The membrane strain in Voigt notation can then be computed as

$$\hat{\varepsilon} = \sum_a \hat{\mathbf{B}}_n^a \mathbf{u}^a \tag{22}$$

where the 3×3 matrix $\hat{\mathbf{B}}_n^a$ is made up of three row vectors:

$$\hat{\mathbf{B}}_n^a := \begin{pmatrix} - & {\mathbf{b}_{n11}^a}^T & - \\ - & {\mathbf{b}_{n22}^a}^T & - \\ - & {\mathbf{b}_{n12}^a}^T + {\mathbf{b}_{n21}^a}^T & - \end{pmatrix} \tag{23}$$

with

$$\mathbf{b}_{n\alpha\beta}^a := \boldsymbol{\varphi}_{0,\alpha} N^a_{,\beta}. \tag{24}$$

Similarly, we write the bending strain in Voigt notation as

$$\hat{\rho} := \begin{pmatrix} \rho_{11} \\ \rho_{22} \\ 2\rho_{12} \end{pmatrix}, \tag{25}$$

which can be computed as

$$\hat{\rho} = \sum_a \hat{\mathbf{B}}_m^a \mathbf{u}^a \tag{26}$$

where the 3×3 matrix $\hat{\mathbf{B}}_m^a$ is made up of three row vectors:

$$\hat{\mathbf{B}}_n^a := \begin{pmatrix} - & {\mathbf{b}_{m11}^a}^T & - \\ - & {\mathbf{b}_{m22}^a}^T & - \\ - & 2{\mathbf{b}_{m12}^a}^T & - \end{pmatrix} \tag{27}$$

with

$$\begin{aligned}
\mathbf{b}_{m\alpha\beta}^a \quad := \quad & \boldsymbol{\varphi}_{0,\alpha\beta} \cdot \mathbf{t}_0 \frac{1}{j_0} \left(N^a_{,1}(\boldsymbol{\varphi}_{0,2} \times \mathbf{t}_0) - N^a_{,2}(\boldsymbol{\varphi}_{0,1} \times \mathbf{t}_0) \right) \\
& + \frac{1}{j_0} \left(N^a_{,1}(\boldsymbol{\varphi}_{0,\alpha\beta} \times \boldsymbol{\varphi}_{0,2}) - N^a_{,2}(\boldsymbol{\varphi}_{0,\alpha\beta} \times \boldsymbol{\varphi}_{0,1}) \right) \\
& - N^a_{,\alpha\beta} \mathbf{t}_0.
\end{aligned} \tag{28}$$

We define the Voigt notation matrix $\hat{\mathbf{H}}$ as

$$\hat{\mathbf{H}} := \begin{pmatrix} \mathcal{H}^{1111} & \mathcal{H}^{1122} & \mathcal{H}^{1112} \\ \mathcal{H}^{2211} & \mathcal{H}^{2222} & \mathcal{H}^{2212} \\ \mathcal{H}^{1211} & \mathcal{H}^{1222} & \mathcal{H}^{1212} \end{pmatrix}, \tag{29}$$

where $\mathcal{H}^{\alpha\beta\gamma\delta}$ is the constitutive tensor defined in (10). The constitutive tensors for membrane and bending stresses (in Voigt notation) can thus be defined as

$$\hat{\mathbf{H}}_n := \frac{Eh}{1-\nu^2}\hat{\mathbf{H}} \tag{30}$$

and

$$\hat{\mathbf{H}}_m := \frac{Eh^3}{12(1-\nu)^2}\hat{\mathbf{H}}. \tag{31}$$

The assembly of an element's membrane stiffness into the global stiffness matrix $\mathbf{K}$ can finally be written as

$$\mathbf{K}^{ab} += \int \hat{\mathbf{B}}_n^{a\,T}\hat{\mathbf{H}}_n\hat{\mathbf{B}}_n^b \mathrm{d}A, \tag{32}$$

where $\mathbf{K}^{ab}$ is the 3×3 block of the stiffness matrix at position (a,b). Similarly, bending stiffness contributions are assembled using

$$\mathbf{K}^{ab} += \int \hat{\mathbf{B}}_m^{a\,T}\hat{\mathbf{H}}_m\hat{\mathbf{B}}_m^b \mathrm{d}A. \tag{33}$$

During the element assembly, (32) and (33) are computed for all pairs of element basis functions a, b for all elements and added to the global stiffness matrix $\mathbf{K}$ as described above.

Edge Contributions. For the computation of edge contributions, a local coordinate system on the edge e is defined as follows: the undeformed normal vector $\mathbf{t}_0^e$ at a point on the edge is set to the normalized average of the adjacent elements' normal vectors at that point, i.e.

$$\mathbf{t}_0^e := \frac{\mathbf{t}_0^+ + \mathbf{t}_0^-}{\|\mathbf{t}_0^+ + \mathbf{t}_0^-\|}. \tag{34}$$

The directed edge is parameterized with $t \in [-1,1]$. A function $\boldsymbol{\xi}_e^+(t) = (\xi_e^{1+}(t), \xi_e^{2+}(t))^T$ determines the position of the edge in local coordinates of element K^+. The first basis vector (along the edge) can thus be defined as

$$\boldsymbol{\varphi}_{0,1}^e := \frac{\partial \boldsymbol{\varphi}_0^+(\boldsymbol{\xi}_e^+(t))}{\partial t} = \boldsymbol{\varphi}_{0,1}^+\frac{\partial \xi_e^{1+}(t)}{\partial t} + \boldsymbol{\varphi}_{0,2}^+\frac{\partial \xi_e^{2+}(t)}{\partial t}. \tag{35}$$

Finally, define

$$\boldsymbol{\varphi}_{0,2}^e := \frac{\mathbf{t}_0^e \times \boldsymbol{\varphi}_{0,1}^e}{\|\mathbf{t}_0^e \times \boldsymbol{\varphi}_{0,1}^e\|}. \tag{36}$$

Note that $\boldsymbol{\varphi}_{0,2}^e$ is equal to the outward unit normal $\boldsymbol{\nu}^-$ of element K^-. Computing $\bar{j}_0$ in this local coordinate system according to (5), it becomes the curve length Jacobian.

The assembly of edge e results in the following contributions to the global stiffness matrix $\mathbf{K}$:

$$\begin{aligned}\mathbf{K}^{ab} \quad += \quad & \int (\tilde{\Delta\mathbf{t}}^{a\pm})^T\hat{\mathbf{N}}^T\hat{\mathbf{H}}_m\hat{\mathbf{N}}\tilde{\Delta\mathbf{t}}^{b\pm}\eta^e\, s^a s^b \mathrm{d}s \\ & + \frac{1}{2}\int (\hat{\mathbf{B}}_m^{a\pm})^T(\hat{\mathbf{H}}_P^{\pm})^T\hat{\mathbf{N}}\tilde{\Delta\mathbf{t}}^{b\pm} s^b \mathrm{d}s \\ & + \frac{1}{2}\int (\tilde{\Delta\mathbf{t}}^{a\pm})^T\hat{\mathbf{N}}\hat{\mathbf{H}}_P^{\pm}\hat{\mathbf{B}}_m^{b\pm} s^a \mathrm{d}s. \end{aligned} \tag{37}$$

Note that $a, b \in B^+ \cup B^-$, where B^+ and B^- are the sets of basis functions used by elements K^+ and K^-, respectively. Depending on which element the basis function is taken from, quantities are either evaluated in K^+ or K^-. $\hat{\mathbf{H}}_P^{\pm}$ is evaluated in the same element as the matrix $\hat{\mathbf{B}}_m^{\pm}$ related to the bending strain. $s^a \in \{-1, 1\}$ assumes a value of 1 if the basis function a is taken from element K^+ and -1 if taken from element K^-.

Note that $\hat{\mathbf{H}}_m$ is evaluated in the local edge coordinate system. $\tilde{\Delta\mathbf{t}}^a$ is related to the change of surface normal and is defined as

$$\begin{aligned}\tilde{\Delta\mathbf{t}}^a \quad := \quad & \frac{1}{\bar{j}_0}([\boldsymbol{\varphi}_{0,1}]_\times - \mathbf{t}_0(\mathbf{t}_0\times\varphi_{0,1})^T)N_{,2}^a \\ & -\frac{1}{\bar{j}_0}([\boldsymbol{\varphi}_{0,2}]_\times - \mathbf{t}_0(\mathbf{t}_0\times\varphi_{0,2})^T)N_{,1}^a \end{aligned} \tag{38}$$

with

$$[\boldsymbol{\varphi}_{0,\alpha}]_\times := \begin{pmatrix} 0 & -\varphi_{0,\alpha}^3 & \varphi_{0,\alpha}^2 \\ \varphi_{0,\alpha}^3 & 0 & -\varphi_{0,\alpha}^1 \\ -\varphi_{0,\alpha}^2 & \varphi_{0,\alpha}^1 & 0 \end{pmatrix}. \tag{39}$$

As the local edge coordinate system is orthogonal and $\boldsymbol{\varphi}_{0,2}^e = \boldsymbol{\nu}^-$ and $\|\boldsymbol{\varphi}_{0,2}^e\| = 1$, it follows that $\nu_1^- = 0$ and $\nu_2^- = 1$. This fact can be used to construct the matrix $\hat{\mathbf{N}}$ as follows:

$$\begin{aligned}\hat{\mathbf{N}} \quad := \quad & \begin{pmatrix} - & \boldsymbol{\varphi}_{0,1}{}^T\nu_1^- & - \\ - & \boldsymbol{\varphi}_{0,2}{}^T\nu_2^- & - \\ - & \boldsymbol{\varphi}_{0,1}{}^T\nu_2^- + \boldsymbol{\varphi}_{0,2}{}^T\nu_1^- & - \end{pmatrix} \\ = \quad & \begin{pmatrix} - & \mathbf{0}^T & - \\ - & \boldsymbol{\varphi}_{0,2}{}^T & - \\ - & \boldsymbol{\varphi}_{0,1}{}^T & - \end{pmatrix}. \end{aligned} \tag{40}$$

$\hat{\mathbf{H}}_P^{\pm}$ represents the push-forward tensors and inverse transformation tensors combined with the constitutive tensor and formulated as a 3×3 matrix in Voigt notation:

$$\hat{\mathbf{H}}_P^{\pm} := (\hat{\mathbf{P}}^{\pm})^T\hat{\mathbf{H}}_m^{\pm}\hat{\mathbf{P}}^{\pm}\hat{\mathbf{p}}^{\pm}, \tag{41}$$

where

$$\hat{\mathbf{P}}^{\pm} := \begin{pmatrix} P_{1111}^{\pm} & P_{1122}^{\pm} & P_{1112}^{\pm} \\ P_{2211}^{\pm} & P_{2222}^{\pm} & P_{2212}^{\pm} \\ 2P_{1211}^{\pm} & 2P_{1222}^{\pm} & P_{1212}^{\pm} + P_{1221}^{\pm} \end{pmatrix} \tag{42}$$

with

$$P_{\alpha\beta\gamma\delta}^{\pm} := (\boldsymbol{\varphi}_0^{,\gamma}\cdot\boldsymbol{\varphi}_{0,\alpha}^{\pm})(\boldsymbol{\varphi}_0^{,\delta}\cdot\boldsymbol{\varphi}_{0,\beta}^{\pm}) \tag{43}$$

and

$$\hat{\mathbf{p}}^{\pm} := \begin{pmatrix} p_{1111}^{\pm} & p_{1122}^{\pm} & p_{1112}^{\pm} \\ p_{2211}^{\pm} & p_{2222}^{\pm} & p_{2212}^{\pm} \\ 2p_{1211}^{\pm} & 2p_{1222}^{\pm} & p_{1212}^{\pm} + p_{1221}^{\pm} \end{pmatrix} \tag{44}$$

with

$$p_{\alpha\beta\gamma\delta}^{\pm} := (\boldsymbol{\varphi}_0^{\pm,\gamma}\cdot\boldsymbol{\varphi}_{0,\alpha})(\boldsymbol{\varphi}_0^{\pm,\delta}\cdot\boldsymbol{\varphi}_{0,\beta}). \tag{45}$$

3.3 Summary

The three main equations for the assembly of the global stiffness matrix are (32), (33), and (37). Fig. 2 shows the main assembly steps in pseudocode.

4 Co-Rotational DG FEM Shells

In its original formulation, the DG FEM treatment of Kirchhoff-Love shells of [Noels and Radovitzky 2008] is not suitable for most graphics applications, because it uses a geometrically linear strain, which results in artifacts in case of large rotational deformations. We therefore propose a simple co-rotational extension that allows arbitrary rotational deformations while still keeping the basic model linear in the displacements.

```
Initialize global stiffness matrix K with zero
for all elements K:
  for all a ∈ B^K:
    for all b ∈ B^K:
      Add membrane contribution (32) to K^ab
      Add bending contribution (33) to K^ab
    end
  end
end
for all interior edges e:
  // Note: Elements adjacent to e are K^+ and K^-
  for all a ∈ B^+ ∪ B^-:
    for all b ∈ B^+ ∪ B^-:
      Add edge contribution (37) to K^ab
    end
  end
end
```

Figure 2: *Summary of stiffness matrix assembly.*

Following [Müller and Gross 2004; Thomaszewski et al. 2006], we compute the strain in an un-rotated coordinate frame and rotate the resulting force back to its original orientation. As components of the same element can deform significantly differently, we apply the co-rotational formulation to each quadrature point i, similar to [Mezger et al. 2008]. For the assembly of element contributions into the global stiffness matrix $\mathbf{K}$ (Equations (32), (33)), numerical quadrature turns the integrals over the elements into per-quadrature point contributions $\mathbf{K}_K^{abi}$:

$$\mathbf{K}^{ab} \mathrel{+}= \mathbf{K}_K^{abi}. \tag{46}$$

Computing the strain in an un-rotated coordinate frame and rotating the resulting force back to its original orientation, the new contributions become

$$\mathbf{K}^{ab} \mathrel{+}= \mathbf{R}^i \, \mathbf{K}_K^{abi} \, \mathbf{R}^{i^T}, \tag{47}$$

$$\mathbf{F}^{a} \mathrel{+}= \mathbf{R}^i \, \mathbf{K}_K^{abi} \, (\mathbf{I} - \mathbf{R}^{i^T}) \, \mathbf{X}_0^b. \tag{48}$$

Note that a corrective term is added to the right-hand side $\mathbf{F}$. $\mathbf{X}_0^b$ is the value for basis function b that reproduces the undeformed configuration. For nodal degrees of freedom, this corresponds to the undeformed position of node b. For additional degrees of freedom such as enrichment functions [Kaufmann et al. 2009], appropriate values for $\mathbf{X}_0^b$ must be defined, following the co-rotational approach for non-nodal basis functions of [Kaufmann et al. 2008]. $\mathbf{R}_i$ is a 3×3 rotation matrix that describes the local rotation at quadrature point i. It can be computed by polar decomposition of the deformation gradient at the quadrature point [Thomaszewski et al. 2006].

The same steps are performed for the edge contributions $\mathbf{K}_e^{abi}$, i.e., for the penalty term that weakly enforces C^1 continuity across edge e. This time, however, the rotation matrix is computed from the deformation gradient in the edge coordinate frame.

5 Results

Fig. 3 shows an example of a nonlinear deformation that would not be possible to simulate using a pure linear deformation model. The cylinder is fixed at both ends and slightly compressed, resulting in a typical buckling deformation. The mesh consists of 961 quad elements and 2945 nodes, with a global stiffness matrix of size 8835×8835.

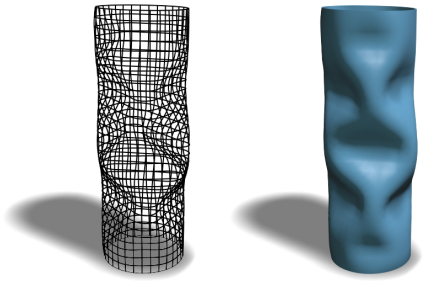

Figure 3: *Co-rotational DG FEM shells allow for the simulation of geometrically-nonlinear phenomena such as buckling (961 quad elements, 2945 nodes).*

6 Conclusion

We have presented an implementation of the linear discontinuous Galerkin shell method of [Noels and Radovitzky 2008] which consistently uses Voigt notation during the stiffness matrix assembly. Our co-rotational extension allows for the simulation of nonlinear phenomena while still being efficient to compute. First tests have shown that DG Shells bear potential for the efficient and realistic simulation of thin objects in computer graphics. The fact that they only require C^0-continuous basis functions greatly simplifies the implementation compared to other finite element methods that also discretize the Kirchhoff-Love shell equations. Furthermore, the reduced continuity requirements are beneficial for discontinuous basis function enrichment [Kaufmann et al. 2009], as they allow the enrichment functions to have discontinuous derivatives across element edges.

Acknowledgments

This work was supported in part by the Swiss National Science Foundation (grant No. 200021-117756) and by the Deutsche Forschungsgemeinschaft (Center of Excellence in "Cognitive Interaction Technology", CITEC).

References

ARNOLD, D. N., BREZZI, F., COCKBURN, B., AND MARINI, L. D. 2001. Unified analysis of discontinuous Galerkin methods for elliptic problems. *SIAM J. Numer. Anal. 39*, 5, 1749–1779.

CIRAK, F., ORTIZ, M., AND SCHRÖDER, P. 2000. Subdivision surfaces: A new paradigm for thin-shell finite-element analysis. *International Journal for Numerical Methods in Engineering 47*, 2039–2072.

HUGHES, T. J. R. 2000. *The Finite Element Method. Linear Static and Dynamic Finite Element Analysis*. Dover Publications.

KAUFMANN, P., MARTIN, S., BOTSCH, M., AND GROSS, M. 2008. Flexible simulation of deformable models using discontinuous Galerkin FEM. In *Proc. of Symp. on Computer Animation*, 105–115.

KAUFMANN, P., MARTIN, S., BOTSCH, M., GRINSPUN, E., AND GROSS, M. 2009. Enrichment textures for detailed cutting of shells. *ACM Trans. on Graphics (Proc. SIGGRAPH) (to appear) 28*, 3.

MEZGER, J., THOMASZEWSKI, B., PABST, S., AND STRASSER, W. 2008. Interactive physically-based shape editing. In *Proc. of ACM Symp. on Solid and Physical Modeling*, 79–89.

MÜLLER, M., AND GROSS, M. 2004. Interactive virtual materials. In *Proc. of Graphics Interface*, 239–246.

NOELS, L., AND RADOVITZKY, R. 2008. A new discontinuous Galerkin method for Kirchhoff-Love shells. *Computer Methods in Applied Mechanics and Engineering 197*, 2901–2929.

SIMO, J. C., AND FOX, D. D. 1989. On stress resultant geometrically exact shell model. Part I: formulation and optimal parametrization. *Computer Methods in Applied Mechanics and Engineering 72*, 3, 267–304.

THOMASZEWSKI, B., WACKER, M., AND STRASSER, W. 2006. A consistent bending model for cloth simulation with corotational subdivision finite elements. In *SCA '06: Proceedings of the 2006 ACM SIGGRAPH/Eurographics symposium on Computer animation*, 107–116.

WEMPNER, G., AND TALASLIDIS, D. 2003. *Mechanics of Solids and Shells: Theories and Approximations*. CRC Press.

ZIENKIEWICZ, O. C., AND TAYLOR, R. 2000. *The Finite Element Method*. Butterworth-Heinemann.